JACS
JOURNAL OF THE AMERICAN CHEMICAL SOCIETY
Article
pubs.acs.org/JACS

Gold as a 6p-Element in Dense Lithium Aurides

Guochun Yang,[†,‡] Yanchao Wang,[†] Feng Peng,[†] Aitor Bergara,[§,∥,⊥] and Yanming Ma*[,†]

[†]State Key Laboratory of Superhard Materials, Jilin University, Changchun 130012, China
[‡]Faculty of Chemistry, Northeast Normal University, Changchun 130024, China
[§]Departmento de Física de la Materia Condensada, Universidad del País Vasco, UPV/EHU, 48080 Bilbao, Spain
[∥]Donostia International Physics Center (DIPC), 20018 Donostia, Spain
[⊥]Centro de Física de Materiales CFM, Centro Mixto CSIC-UPV/EHU, 20018 Donostia, Spain

Supporting Information

ABSTRACT: The negative oxidation state of gold (Au) has drawn a great attention due to its unusual valence state that induces exotic properties in its compounds, including ferroelectricity and electronic polarization. Although monatomic anionic gold (Au^-) has been reported, a higher negative oxidation state of Au has not been observed yet. Here we propose that high pressure becomes a controllable method for preparing high negative oxidation state of Au through its reaction with lithium. First-principles calculations in combination with swarm structural searches disclosed chemical reactions between Au and Li at high pressure, where stable Li-rich aurides with unexpected stoichiometries (e.g., Li_4Au and Li_5Au) emerge. These compounds exhibit intriguing structural features like Au-centered polyhedrons and a graphene-like Li sublattice, where each Au gains more than one electron donated by Li and acts as a 6p-element. The high negative oxidation state of Au has also been achieved through its reactions with other alkali metals (e.g., Cs) under pressures. Our work provides a useful strategy for achieving diverse Au anions.

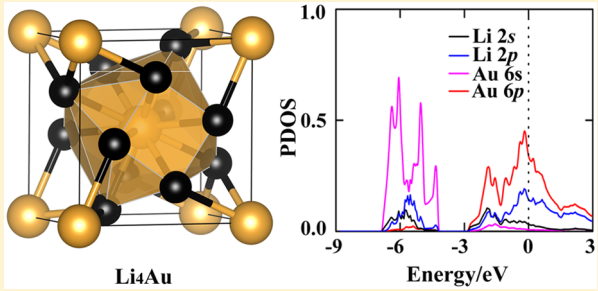

1. INTRODUCTION

Au is a well-known fascinating element but still hides interesting surprises to be discovered.[1−4] It is used in coinage and ornament because of its extreme inertness at ambient conditions. However, gold has a rich chemistry under certain conditions and can form diverse compounds that have many uses in medicine,[5] catalysis,[6,7] electron transport,[8] luminescence,[9] nonlinear optics,[10] and electronics.[11] Notably, the chemical properties of gold, in some aspects, are different from that of the other metals, and the main differences are the consequence of the relativistic effects.[12−16] The expansion of the 5d orbital favors the formation of +3 or higher (e.g., + 5) oxidation states in Au.[12] As such, the closed shell $5d^{10}$ of Au opens up, and Au becomes chemically reactive with other elements in molecules or clusters.[17] Aurophilic interactions, originated from relativistic effects and electronic correlation of closed-shell components,[18,19] defined as intra- and intermolecular bonding between Au^+ centers, greatly affect molecular and crystal structures of Au compounds, leading to unusual chemical and physical properties.[20,21]

The contraction of the 6s orbital, however, makes Au have the highest electronegativity among all metals and enhances its trend to present a negative oxidation state.[14] To the best of our knowledge, the only known negative oxidation state of Au is Au^-, with an electron configuration $5d^{10}6s^2$,[14] that is, isoelectronic with Hg, Tl^+, and Pb^{2+}. Many exotic chemical and physical properties, resulted from the appearance of 6*s* lone electron pair, have been observed.[22−24] For example, high polarizability associated with the presence of lone electron pairs can induce high dielectric constants, large Born effective charges, ferroelectricity, and large longitudinal and transverse-optical phonon splittings.[22] Additionally, a 6s electron of Au^- can be easily promoted into the 6p level, showing, therefore, a mixed shell configuration of 6s + 6p.[14] Even aurophilic attraction that was observed between Au^+ cations can emerge between Au^- anions.[12] The observation of all of these features has generated great interest in the chemistry of Au^- compounds. Till now, many compounds containing Au^- have been found: CsAu,[25,26] $Rb_8AlO_4Au_3$,[27] A_3AuO (A = Rb, Cs),[28] and others.[29] These compounds show interesting structural and electronic properties.[14,30−32]

It is worth mentioning that all of these compounds consisted of Au^- anions have been synthesized just at or near ambient pressure. It is now well-accepted that high pressure has become an irreplaceable tool to discover new materials with exciting chemical properties.[33−35] The application of pressure can overcome activation barriers for chemical reactions,[36] reorder atomic orbital energy levels,[37] induce structural phase transitions,[38] and modify electronic properties.[39] Many unusual stoichiometric compounds with exotic chemical properties that are not accessible at ambient pressure have been discovered

Received: November 10, 2015
Published: March 4, 2016

© 2016 American Chemical Society

DOI: 10.1021/jacs.5b11768
J. Am. Chem. Soc. 2016, 138, 4046−4052

under high pressure.[40−47] These findings are greatly benefitted from the recent application of first-principles structural prediction methods[48−51] that are particularly successful in the identification of unusual stoichiometric materials under high pressure. For instance, the predicted $NaCl_3$ and Na_3Cl compounds under high pressure have been confirmed experimentally.[40]

Previous studies have identified that alkali metals show a clear orbital hybridization (e.g., s−p, s−d, or p−d electronic transitions) under pressure, which strongly modifies their chemical reactivities.[52−55] There is an expectation on the formation of unusual stoichiometric alkali metals aurides under pressure that are out of reach at ambient pressure.[56,57] Moreover, the electronegativity of lithium (Li) is much smaller than that of Au. When Li is alloyed with Au, they are subject to obviously positive and negative polarization.[14] Once particular Li−Au alloys are stabilized under high pressure, one might anticipate the formation of higher negative oxidation state (> −1) in Au, a chemical state that is unforeseen at ambient pressure.

In an effort to pursue higher negative oxidation state of Au, we here conduct an extensive structure study on stable Li−Au compounds with various Li_nAu_m (n = 1−6 and m = 1, or n = 1 and m = 1−6) compositions under pressure by using the swarm-intelligence based first-principles structural prediction calculations.[48,49] In addition to the known $LiAu_3$, LiAu, and Li_3Au, unusual stoichiometric Li_4Au and Li_5Au compounds are unraveled and found to be stable under high pressure. In these Li-rich compounds, Au is in > −1 state by receiving more than one electron from Li, and it behaves as a 6p-element, having a $5d^{10}6s^26p^n$ ($n \geq 1$) electronic configuration. Moreover, the negative oxidation states of Au can be effectively tuned from −1 to −3 (or even higher) by varying the Li compositions at certain pressures.

2. COMPUTATIONAL METHODS AND DETAILS

In order to analyze the preferred structures of Li−Au at high pressures, we have used the swarm-intelligence based CALYPSO structure prediction method, which searches for the stable structures of given compounds.[48,49] CALYPSO can find the most stable structures just knowing the chemical composition; therefore, it is unbiased by already known structures. CALYPSO has been validated with various known systems, ranging from elements to binary and ternary compounds.[37,46,58,59] Detailed descriptions of the method and structural predictions can be found in the Supporting Information.

Total energy calculations are performed in the framework of density functional theory within the generalized gradient approximation[60] as implemented in the VASP code.[61] The electron−ion interaction is described by pseudopotentials built within the scalar relativistic projector augmented wave approximation with s^1p^0 and $5d^{10}6s^1$ valence electrons for Li and Au atoms, respectively. A cutoff energy of 700 eV and appropriate Monkhorst−Pack k-meshes are used to ensure that total energy calculations are converged to less than 1 meV/atom. The thermodynamical stability of different Li−Au compounds with respect to elemental Li and Au solids at each pressure is evaluated through the below equation:[62,63]

$$\Delta G_f(Li_nAu_m) = [G(Li_nAu_m) - nG(Li) - mG(Au)]/(m + n) \quad (1)$$

where $G = U + PV - TS$ is the Gibbs free energy of each composition and ΔG_f is the Gibbs free energy of formation per atom. Here, U, P, V, T, and S are the internal energy, pressure, volume, temperature, and entropy, respectively. Note that G reduces to the enthalpy ($H = U + PV$) at T = 0 K.[64] To determine the dynamical stability of predicted structures, the phonon calculations were performed by using the finite displacement approach as implemented in the Phonopy code.[65] The validity of pseudopotentials used at high pressures is examined with the full-potential linearized augmented plane-wave method as implemented in the WIEN2k package.[66] See Supporting Information for more details.

3. RESULTS AND DISCUSSION

3.1. Phase Stabilities and Structures of Li−Au Compounds. We have performed extensive structural searches on Li−Au compounds for various Li_nAu_m (n = 1−6 and m = 1, or n = 1 and m = 1−6) compositions at 0 K and selected pressures of 0, 25, 50, and 100 GPa. The predicted structure for each composition is then used to evaluate Gibbs free energy of formation (ΔG_f) relative to elemental Li and Au solids according to eq 1. Convex hull data at 0 K for Li−Au system with variation of compositions at different pressures are constructed and presented in Figure 1 by evaluating the

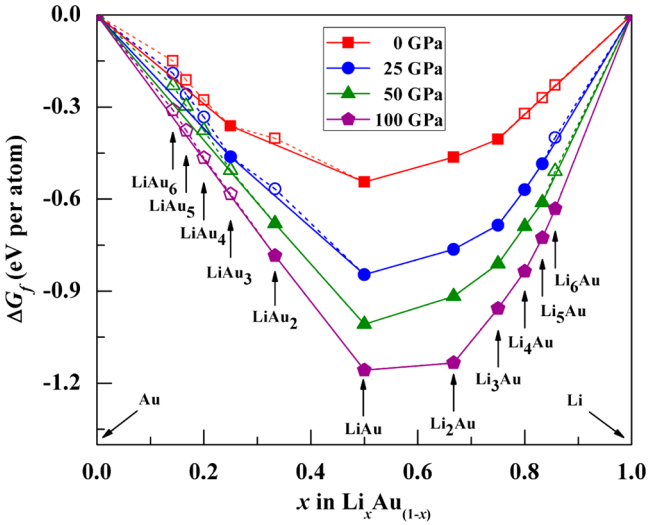

Figure 1. Phase stabilities of various Li_nAu_m (n = 1−6 and m = 1, or n = 1 and m = 1−6) compounds with respect to elemental Li and Au solids at 0 K. The convex hulls are shown with solid lines. Dotted guidelines directly connect the data points. Compounds corresponding to data points located on the convex hull are thermodynamically stable. The phases I (bcc), II (fcc), IV ($cI16$), and VI ($oC24$) of solid Li,[54,69] and the face centered cubic structure (Fm-3m) of solid Au[70] are used to calculate Gibbs free energy of formation.

averaged ΔG_f for each composition. According to the hull data, a compound with a ΔG_f lying on the convex hull is thermodynamically stable with respect to decomposition into other Li−Au compounds or elemental Li and Au solids, and thus, it is experimentally synthesizable.[67] At 0 GPa, the already known $LiAu_3$, LiAu, and Li_3Au phases are readily identified in our calculations,[68] validating our structure searching method when applied to the Li−Au system. Besides, we predicted the stabilization of a new Li_2Au compound that was not previously reported, awaiting future experimental synthesis. Our calculated lattice parameters for Li_3Au (space group Fm-3m, 4 formula units per cell) is 6.31 Å, in excellent agreement with the experimental value at 6.30 Å.[68]

At elevated pressures, it is exciting to note that more Li-rich compositions of Li_4Au and Li_5Au appear to be stable at 25 and 50 GPa, and the highest Li-rich composition, Li_6Au, is stabilized at 100 GPa. Beside $LiAu_3$, $LiAu_2$ is the only new stable stoichiometry identified in the Au-rich region at 50 and 100 GPa. It should be pointed out that all of the stable Li−Au

DOI: 10.1021/jacs.5b11768
J. Am. Chem. Soc. 2016, 138, 4046−4052

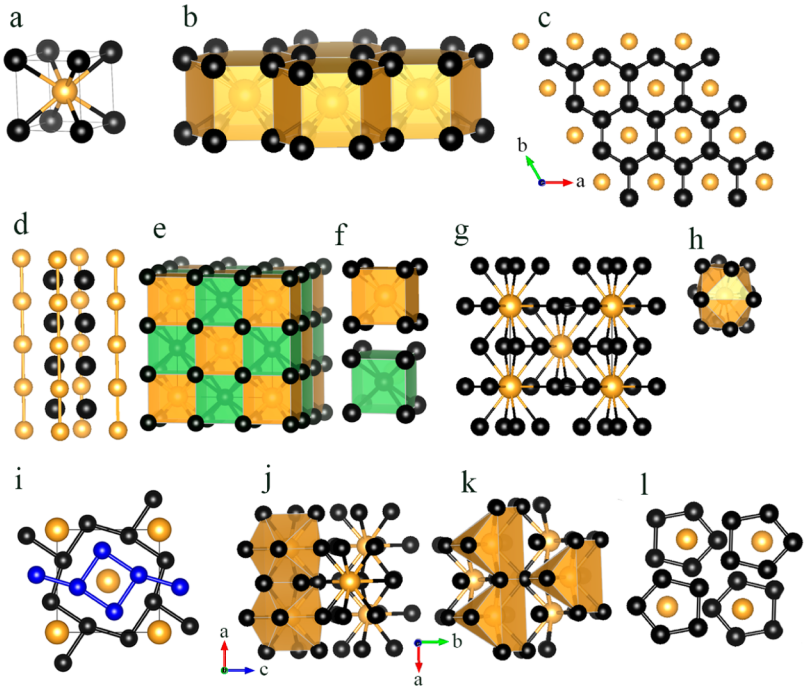

Figure 2. Stable structures of Li_nAu (n = 1−5) at 50 GPa. The lattice parameters of all of the structures are listed in the Supporting Information (Table S1). (a) LiAu in the *Pm*-3*m* structure. (b) Li_2Au in the *P6*/*mmm* structure. (c) A Li graphene-like layered structure in the *P6*/*mmm* structure of Li_2Au. (d) Linear Au chains in the *P6*/*mmm* structure of Li_2Au. (e) Li_3Au in the *Fm*-3*m* structure. (f) View of hexahedrons in Li_3Au. (g) Li_4Au in the *I*4/*m* structure. (h) View of a dodecahedron in Li_4Au. (i) Square Li_4 and octagonal Li_8 rings in the *I*4/*m* structure of Li_4Au. (j and k) Li_5Au in the *Cmcm* structure. (l) Planar five-membered Li_5 pentagonal rings in the *Cmcm* structure of Li_5Au. In all the structures, small black or blue and large golden spheres represent Li and Au atoms, respectively.

compounds predicted undergo a series of structural phase transitions under pressure (Table S1). We have examined the effect of temperature on the phase stability (Figure S1) based on the quasi-harmonic approximation calculations.[65] All of the stable phases predicted at 0 K remain stable at the elevated temperatures of 500 and 1000 K.

Despite the differences in composition and symmetry, crystal structures of Li_nAu (n > 1) compounds exhibit quite similar Li−Au bonding patterns. To compare the structural variations for the different stoichiometries, we mainly analyze Li_nAu (n = 1−5) structures at 50 GPa (Figure 2). The nearest Li−Li, Li−Au, and Au−Au distances in Li_nAu (n = 1−5) are given in Figure S2. For comparison, Li−Li and Au−Au distances in their element solids are also included. LiAu adopts a well-known CsCl-type structure appearing in many ionic compounds (Figure 2a). Li_2Au has a MgB_2-type structure (space group *P6*/*mmm*, 1 formula unit per cell; Figure 2b) consisting of face-sharing Au−Li octahedrons. There, Li atoms form an interesting graphene-like layered structure in the *ab* plane (Figure 2c), while Au atoms form one-dimensional chains along the *c*-axis with equal Au−Au distance of 2.64 Å (Figure 2d), which is slightly longer than that in the Au dimer (2.47 Å)[71] and much shorter than the aurophilic interaction distances: 3.0 Å for $Au^{+}\cdots Au^{+}$[72] and 3.02 Å for $Au^{-}\cdots Au^{-}$.[12] Li_3Au stabilizes into a BiF_3-type structure (space group *Fm*-3*m*, 4 formula units per cell; Figure 2e). As it can be seen in Figure 2f, basic building blocks of the structure are square Li cages with alternating Li/Au atoms at the center. Unlike Li_2Au, the distance between the two nearest Au atoms is much enlarged (3.77 Å) and significantly longer than the aurophilic interaction distance. Thus, Au−Au interaction in Li_3Au becomes much weaker, which is also supported by the result of the integrated crystal orbital Hamilton populations (ICOHPs),[73] as will be discussed below. Li_4Au adopts a tetragonal structure (space group *I*4/*m*, 4 formula units per cell; Figure 2g). For each Au atom, there are 12 nearest neighbors of Li atoms, forming a Au−Li tetradecahedron (Figure 2h). When compared with Li_3Au, the distance between the two nearest Au atoms becomes even larger (3.94 Å). Nearest-neighbor Li atoms form both square Li_4 and octagonal Li_8 rings (Figure 2i). Li_5Au stabilizes into an orthorhombic structure (space group *Cmcm*, 2 formula units per cell; Figure 2j). Each Au is surrounded by nine nearest neighbors of Li atoms to form a quasi-tricapped trigonal geometry (Figure 2k), which has been observed in rhenium complexes, such as $[ReH_9]^{2-}$[74] and its derivatives.[75] The nearest Li atoms form a five-membered ring (Figure 2l). Again, the nearest Au−Au distance is 3.71 Å, which is larger than the aurophilic interaction distance.

All of the structures of Li-rich aurides we have studied under pressure, Li_nAu (n = 1−5), show Au enclosed by Li atoms in different Au−Li polyhedrons (Figures 2 and S3). Rising Li content shortens Li−Au distances but enlarges the separation between the two nearest Au atoms (Figures S2−5). Interestingly, in Li-rich aurides, Au−Au distances are much longer than the aurophilic interaction distance, and Li atoms show various ring shapes or sheet patterns, similar to those observed in alkali metal suboxides,[76] subhydrides,[77] and Li_nCs compounds.[78] As it will be discussed below, short bond lengths in these compounds lead to strong interatomic interactions, which play an important role in stabilizing the structures.

3.2. Electronic Structures and Chemical Bonds. To understand the nature of the chemical bonding and the formation mechanism of these various Li−Au compounds, we have calculated their electronic band structures and projected

DOI: 10.1021/jacs.5b11768
J. Am. Chem. Soc. 2016, 138, 4046−4052

density of states (PDOS). As can be seen in Figure 3a, Li_5Au shows a pronounced Au 6p component below the Fermi level.

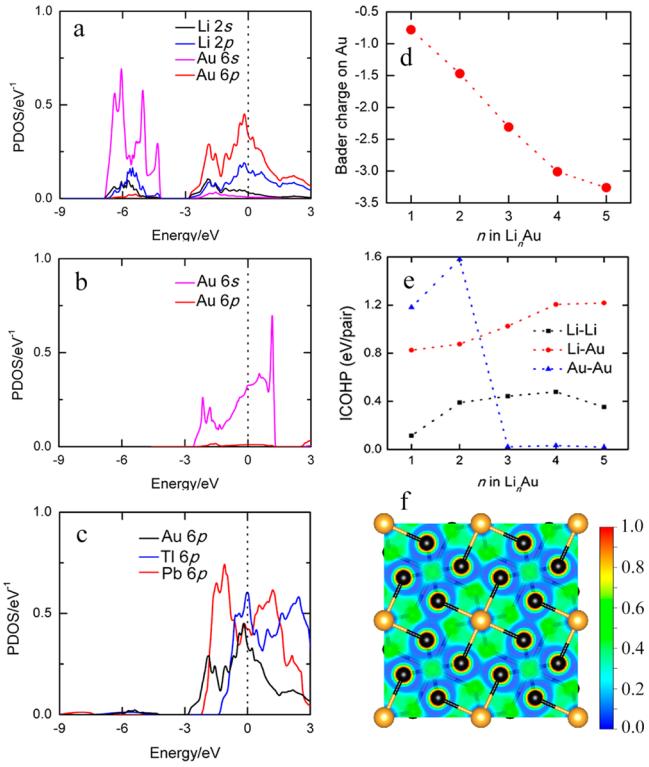

Figure 3. Electronic structures and Li−Au bonding of Li−Au compounds at 50 GPa. (a) PDOS calculated using the Perdew−Burke−Ernzerhof functional for Li_5Au in the *Cmcm* structure. The PDOS of Au 5d is not included here for clarity and is instead given in Figure S5. The dashed line indicates the Fermi energy. The PDOS reveals the metallic nature of Li−Au compounds. (b) The PDOS of Au in Li_0Au with the *Cmcm* structure. (c) The occupation of the 6p state of Au in Li_5Au within the *Cmcm* structure is compared with those of 6p states for Tl and Pb as modeled by Li_0Tl and Li_0Pb. The current comparison unambiguously shows that Au in Li_5Au acts as a 6p-block element, similar to Tl and Pb elements. (d) The Bader charge of Au in various Li_nAu (n = 1−5) compounds, showing that the negative oxidation state of Au is beyond −3 in Li_4Au and Li_5Au. (e) Calculated integrated crystal orbital Hamiltonian populations (ICOHP) for Li−Li, Li−Au, and Au−Au pairs in Li_nAu compounds. Positive ICOHP values represent bonding states. (f) Calculated ELF for Li_4Au on the (001) plane in the $I4/m$ structure.

The analysis of electronic states around the Fermi level shows that there is a large overlap between Au 6p and Li 2s or 2p, indicating that a charge transfer can occur from Li 2s and 2p to Au 6p. To confirm this, we have constructed a hypothetical model system of Li_0Au, in which all Li atoms are removed from the Li_5Au structure. The calculated PDOS of Li_0Au is presented in Figure 3b. The absence of 6p electrons and the presence of partially occupied 6s electrons in the hypothetical Li_0Au confirms that Au atoms indeed gain electrons from Li in Li_5Au. This charge transfer is further supported by the difference charge density analysis (Figure. S9).

The PDOS of the other Li_nAu (n = 1−4) compounds show that Li composition greatly affects the associated charge transfer. Specifically, increasing Li content leads to an increasing Au 6s and 6p contributions below the Fermi level (the green and black lines in Figure S10), indicating that the Li → Au charge transfer can be effectively tuned by controlling Li composition. Note that Au 6s orbitals are completely filled, especially when n is greater than or equal to 3 (Figure S11). Another interesting trend in the PDOS is that Au 5d states become localized and exhibit stronger isolated atomic orbital features (Figure S12) with increasing Li content, which is consistent with the isolated Au atom in the Li matrix. The PDOS shows that Au 5d and 6p orbitals are separated each other without having any 5d−6p orbital hybridization. This is in sharp contrast to the situation of orbital hybridization between Au 6p and Au 5d or 6s in Li_3Au at ambient conditions (Figure S13). Similar results are observed for Li−Au compounds at 100 GPa (Figure S14).

To illustrate the charge transfer between Li and Au, the Bader charge analysis has been considered, which is calculated by partitioning the space into Bader basins around each atom based on stationary points in the charge density.[79] Integration of the charges in each basin gives the total charge associated with each atom. For ease of comparison, the Bader charge analysis of Li_nAu (n = 1−5) compounds at 50 GPa (red line in Figure 3d) was calculated. The Bader charge on Au increases in magnitude (becoming more negative) almost linearly with increasing the Li composition, indicating that the negative oxidation state of Au can be effectively tuned by controlling Li composition. Actually, the large charge transfer from Li to Au is the major driven force stabilizing Li_nAu (n = 1−5) compounds. The accepted charges of Au mainly fill Au 6s and 6p orbitals. It is noteworthy that Bader charge analysis often underestimates the formal oxidation states for ionic compounds. For example, the Bader charge of Cs in an ideal ionic crystal of CsF is +0.81, instead of +1.[37] However, even considering Bader charges, the negative oxidation state of Au is already larger than −3 in Li_nAu ($n \geq 4$) compounds, unambiguously demonstrating that Au acts as a p-block element. Using *Cmcm*-structured Li_5Au as a parent structure, we further constructed two other model systems of Li_0Tl and Li_0Pb by removing all Li atoms out of the lattic and replacing Au with Tl and Pb, respectively. This allows us to have a direct comparison on the PDOS of 6p state of Au in Li_5Au with those of 6p states of Tl and Pb in Li_0Tl and Li_0Pb (Figure 3c). This comparison gives a solid support on that Au atom in Li_5Au has the characteristics of a 6p element.

Since charge transfer from Li to Au in Li_nAu (n = 1−5) compounds is high, strong interaction between Li and Au atoms is expected, which is examined by calculating their respective integrated crystal orbital Hamilton populations (ICOHPs)[73] using the linear muffin-tin orbital method. The ICOHP can be scaled with the bond strength in compounds by counting the energy weighted population of wavefunctions between two atomic orbitals. Figure 3e shows that the ICOHP between Li−Au and Li−Li pairs becomes larger with increasing Li composition, indicating the strengthening of Li−Au and Li−Li interactions. However, the ICOHP between Au−Au pairs exhibits the opposite trend. The large variation of Au−Au interactions for LiAu and Li_2Au away from the general trend of the ICOHP is probably caused by their very short Au−Au distances (2.787 and 2.639 Å, respectively), showing strong Au−Au interactions. With increasing Li composition, the coordination number of Au also increases, making Li−Au interaction mainly responsible for the structural stability in Li_nAu ($n \geq 3$). The decomposition of ICOHP into atomic orbitals indicates that the main contributions for Li−Au pairs are between Li 2p and Au 6s or 6p orbitals. For example, the ICOHP of Li−Au can be as large as 1.22 eV per pair in Li_5Au at 50 GPa, and its major contributions come from 2p−6s, 2p−6p,

DOI: 10.1021/jacs.5b11768
J. Am. Chem. Soc. 2016, 138, 4046−4052

2s−6p, 2s−6s, and 2s−5d, which correspond to decomposed ICOHP of 0.27, 0.30, 0.17, 0.14, and 0.24 eV per pair, respectively.

Electron localization function (ELF) maps the probability of finding electrons in different areas of a crystal.[80,81] Large values (>0.5) generally correspond to covalent bonds and inner shell or lone pair electrons, whereas ionic and metallic bonds are represented by smaller ELF values. Figure 3f shows large areas with small ELF values (approximately 0.38) between Li and Au atoms, which is typical of ionic bonding.[82] The largest observed ELF values near Li atoms are associated with 1s core electrons.

3.3. The Formation Mechanism of Stable Li−Au Compounds. The potential of Au to adopt high negative oxidation state is demonstrated by the variations of atomic orbital energy levels for Li and Au atoms under pressure (Figure 4). Under ambient conditions, Au 6s energy level is lower than Li 2s; however, the Au 6p orbital energy level is much higher than Li 2s. Thus, at normal conditions Li 2s orbital is not mixed with Au 6p. Under pressure Li 2s and 2p orbital energy levels rise much faster than Au 6p, overpassing it. This feature facilitates a flow of Li 2s or 2p electrons to Au 6p, reducing the total energy, so that Li_nAu compounds become stable; which also helps us to understand why there are more stable Li-rich stoichiometries than Au-rich ones, as shown in Figure 1. It is noted that Au 6p atomic orbital might be fairly diffuse, so that one could not exclude the alternative possibility of electron occupation in a linear combination between Au 6p and Li 2s or 2p.[83] In addition, the energy difference between Au 5d and Au 6s or 6p orbitals becomes larger with increasing pressure, which do not favor any orbital hybridization between them, as can be deduced from the resulting highly localized Au 5d orbital (Figure S12). It is very similar to what happens in Na_6Hg_4 and Na_2Hg_3, where 5d electrons can be considered as part of the core.[84,85]

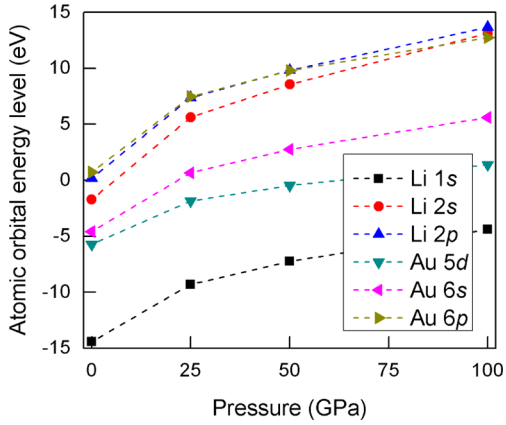

Figure 4. Atomic orbital energy levels for Li and Au atoms as a function of the external pressure. Pressure effect is modeled by putting elements in a face-centered cubic (fcc) He matrix. A fcc supercell of 108 He (3 × 3 × 3) is used, in which one He atom is replaced by the atom being examined. Li 2s and 2p energy levels overpass the Au 6p energy level, indicating Au can gain more than one electron from Li at high enough pressures.

To gain a complete overview on alkali metal aurides, we have also checked the possibility of alloying Au with other alkali metals under high pressure. Having in mind that Cs has the lowest electronegativity among Li, Na, K, Rb, and Cs, it has been chosen as the bottom end element to investigate its reactions with Au under high pressure. According to our calculations, it is found that Cs-rich compounds (i.e., Cs_3Au) appear to be stable at 25 GPa (Figure S15). The analysis of the electronic charges shows that Cs_3Au exhibits a similar charge transfer as the one observed in Li−Au compounds, and Au in Cs_3Au also behaves as a 6p-block element (detailed information can be found in the Supporting Information). Therefore, we expect that it is a general behavior on formation of alkali metal aurides under high pressures where Au behaves as a p-element. However, large differences (i.e., reaction pressures, crystal structures, and pressure-related structure stabilities) can also be expected between different alkali metal aurides, as originated from intrinsic differences between the alkali metals. For instance, when pressure is above 100 GPa, all of the considered Cs−Au compounds tend to decompose into elemental solids. This phase instability is completely different from what is observed in Li−Au compounds showing phase stabilities to a great extent of pressure, which can be understood by considering the different variations of the orbital energy levels of Li (Figure 4) and Cs (Figure S16) atoms under pressure. It is found that when pressure is below 35 GPa, the orbital energy levels of Cs 6s and 6p are higher than Au 6p, which favors the charge transfer from Cs to Au and reduces the energy stabilizing Cs−Au compounds. However, when pressure goes above 35 GPa, the opposite behavior is observed.

4. CONCLUSION

Unbiased structure searching and density functional total energy calculations were performed to explore phase stabilities and crystal structures of Li−Au compounds under high pressures in an effort to achieve high negative oxidation states of Au. We find Au is able to react with Li at experimentally accessible pressures by forming various intermetallic Li−Au compounds. In Li-rich aurides Au gains electrons and presents high negative oxidation states, which range from −1 to −3 (or above), having a $5d^{10}6s^26p^n$ ($n \geq 1$) electron configuration and, therefore, acts as a true p-element. The underlying mechanism of this feature is the different pressure-induced shifting of atomic orbital energy levels. Under reasonably high pressures, Au can also form intermetallic compounds with other alkali metals (i.e., Cs), where Au also behaves as a p-element. According to our results, applying pressure becomes a controllable method for achieving unusual negative oxidation states of Au in alkali metal aurides.

■ ASSOCIATED CONTENT

Supporting Information

The Supporting Information is available free of charge on the ACS Publications website at DOI: 10.1021/jacs.5b11768.

Detailed description of the calculation method and structural predictions, main structural parameters, electron energy band structure, phonon dispersion curve, PDOS, and main results of Cs−Au compounds (PDF)

■ AUTHOR INFORMATION

Corresponding Author

*mym@jlu.edu.cn,mym@calypso.cn

Notes

The authors declare no competing financial interest.

DOI: 10.1021/jacs.5b11768
J. Am. Chem. Soc. 2016, 138, 4046−4052

■ ACKNOWLEDGMENTS

This research was supported by Natural Science Foundation of China under Nos. 21573037, 11274136, and 11534003, the 2012 Changjiang Scholars Program of China, the Postdoctoral Science Foundation of China under grant 2013M541283, the Natural Science Foundation of Jilin Province (20150101042JC), the Department of Education, Universities and Research of the Basque Government and the University of the Basque Country (IT756-13), and the Ministerio de Economía y Competitividad through grants no. FIS2013-48286-C2-1-P and FIS2013-48286-C2-2-P.

■ REFERENCES

(1) Dorel, R.; Echavarren, A. M. *Chem. Rev.* **2015**, *115*, 9028.
(2) Qin, Z.; Bischof, J. C. *Chem. Soc. Rev.* **2012**, *41*, 1191.
(3) Hutchings, G. J.; Brust, M.; Schmidbaur, H. *Chem. Soc. Rev.* **2008**, *37*, 1759.
(4) Yang, X.; Yang, M. X.; Pang, B.; Vara, M.; Xia, Y. N. *Chem. Rev.* **2015**, *115*, 10410.
(5) Johnson, B. T.; Low, R. E.; MacDonald, H. V. *Psychol. Health.* **2015**, *30*, 135.
(6) Guenther, J.; Mallet-Ladeira, S.; Estevez, L.; Miqueu, K.; Amgoune, A.; Bourissou, D. *J. Am. Chem. Soc.* **2014**, *136*, 1778.
(7) Rudolph, M.; Hashmi, A. S. K. *Chem. Soc. Rev.* **2012**, *41*, 2448.
(8) Kodiyath, R.; Manikandan, M.; Liu, L.; Ramesh, G. V.; Koyasu, S.; Miyauchi, M.; Sakuma, Y.; Tanabe, T.; Gunji, T.; Duy Dao, T.; Ueda, S.; Nagao, T.; Ye, J.; Abe, H. *Chem. Commun.* **2014**, *50*, 15553.
(9) Au, V. K.-M.; Wong, K. M.-C.; Zhu, N.; Yam, V. W.-W. *J. Am. Chem. Soc.* **2009**, *131*, 9076.
(10) Aragoni, M. C.; Arca, M.; Devillanova, F. A.; Isaia, F.; Lippolis, V.; Pintus, A. *Chem. - Asian J.* **2011**, *6*, 198.
(11) Holliday, R.; Goodman, P. *Iee. Review.* **2002**, *48*, 15.
(12) Gimeno, M. C.; Laguna, A. *Gold. Bull.* **2003**, *36*, 83.
(13) Jiang, D. E.; Walter, M. *Phys. Rev. B: Condens. Matter Mater. Phys.* **2011**, *84*, 193402.
(14) Jansen, M. *Chem. Soc. Rev.* **2008**, *37*, 1826.
(15) Pyykko, P. In *Annu. Rev. Phys. Chem.*; Johnson, M. A., Martinez, T. J., Eds.; **2012**; Vol. *63*, p 45.10.1146/annurev-physchem-032511-143755
(16) Pyykko, P. *Angew. Chem., Int. Ed.* **2004**, *43*, 4412.
(17) Sunick, D. L.; White, P. S.; Schauer, C. K. *Angew. Chem., Int. Ed. Engl.* **1994**, *33*, 75.
(18) Pyykko, P.; Zhao, Y. F. *Angew. Chem., Int. Ed. Engl.* **1991**, *30*, 604.
(19) Pyykko, P. *Chem. Soc. Rev.* **2008**, *37*, 1967.
(20) Schmidbaur, H.; Schier, A. *Chem. Soc. Rev.* **2012**, *41*, 370.
(21) Schmidbaur, H.; Schier, A. *Chem. Soc. Rev.* **2008**, *37*, 1931.
(22) Miao, M.; Brgoch, J.; Krishnapriyan, A.; Goldman, A.; Kurzman, J. A.; Seshadri, R. *Inorg. Chem.* **2013**, *52*, 8183.
(23) Walsh, A.; Payne, D. J.; Egdell, R. G.; Watson, G. W. *Chem. Soc. Rev.* **2011**, *40*, 4455.
(24) Du, M. H.; Singh, D. J. *Phys. Rev. B: Condens. Matter Mater. Phys.* **2010**, *81*, 144114.
(25) Sommer, A. *Nature* **1943**, *152*, 215.
(26) Spicer, W. E.; Sommer, A. H.; White, J. G. *Phys. Rev.* **1959**, *115*, 57.
(27) Mudring, A.-V.; Jansen, M. *Z. Naturforsch., B: J. Chem. Sci.* **2001**, *56*, 433.
(28) Pantelouris, A.; Kueper, G.; Hormes, J.; Feldmann, C.; Jansen, M. *J. Am. Chem. Soc.* **1995**, *117*, 11749.
(29) Köhler, J.; Whangbo, M. H. *Chem. Mater.* **2008**, *20*, 2751.
(30) Sarmiento-Pérez, R.; Cerqueira, T. F. T.; Valencia-Jaime, I.; Amsler, M.; Goedecker, S.; Botti, S.; Marques, M. A. L.; Romero, A. H. *New J. Phys.* **2013**, *15*, 115007.
(31) Ferro, R.; Saccone, A.; Macciò, D.; Delfino, S. *Gold. Bull.* **2003**, *36*, 39.
(32) Ellis, J. E. *Inorg. Chem.* **2006**, *45*, 5710.
(33) McMillan, P. F. *Chem. Soc. Rev.* **2006**, *35*, 855.
(34) Wang, Y. C.; Ma, Y. M. *J. Chem. Phys.* **2014**, *140*, 040901.
(35) Wang, Y. C.; Lv, J.; Zhu, L.; Lu, S. H.; Yin, K. T.; Li, Q.; Wang, H.; Zhang, L. J.; Ma, Y. M. *J. Phys.: Condens. Matter* **2015**, *27*, 203203.
(36) Zurek, E.; Hoffmann, R.; Ashcroft, N. W.; Oganov, A. R.; Lyakhov, A. O. *Proc. Natl. Acad. Sci. U. S. A.* **2009**, *106*, 17640.
(37) Miao, M. S. *Nat. Chem.* **2013**, *5*, 846.
(38) Ma, Y. M.; Eremets, M.; Oganov, A. R.; Xie, Y.; Trojan, I.; Medvedev, S.; Lyakhov, A. O.; Valle, M.; Prakapenka, V. *Nature* **2009**, *458*, 182.
(39) McWilliams, R. S.; Spaulding, D. K.; Eggert, J. H.; Celliers, P. M.; Hicks, D. G.; Smith, R. F.; Collins, G. W.; Jeanloz, R. *Science* **2012**, *338*, 1330.
(40) Zhang, W.; Oganov, A. R.; Goncharov, A. F.; Zhu, Q.; Boulfelfel, S. E.; Lyakhov, A. O.; Stavrou, E.; Somayazulu, M.; Prakapenka, V. B.; Konopkova, Z. *Science* **2013**, *342*, 1502.
(41) Miao, M. S.; Wang, X. L.; Brgoch, J.; Spera, F.; Jackson, M. G.; Kresse, G.; Lin, H. Q. *J. Am. Chem. Soc.* **2015**, *137*, 14122.
(42) Pinkowicz, D.; Rams, M.; Misek, M.; Kamenev, K. V.; Tomkowiak, H.; Katrusiak, A.; Sieklucka, B. *J. Am. Chem. Soc.* **2015**, *137*, 8795.
(43) Peng, F.; Miao, M. S.; Wang, H.; Li, Q.; Ma, Y. M. *J. Am. Chem. Soc.* **2012**, *134*, 18599.
(44) Wang, H.; Tse, J. S.; Tanaka, K.; Iitaka, T.; Ma, Y. M. *Proc. Natl. Acad. Sci. U. S. A.* **2012**, *109*, 6463.
(45) Botana, J.; Wang, X. Q.; Hou, C. J.; Yan, D. D.; Lin, H. Q.; Ma, Y. M.; Miao, M. S. *Angew. Chem., Int. Ed.* **2015**, *54*, 9280.
(46) Zhu, L.; Liu, H.; Pickard, C. J.; Zou, G.; Ma, Y. *Nat. Chem.* **2014**, *6*, 644.
(47) Zhong, X.; Wang, H.; Zhang, J. R.; Liu, H. Y.; Zhang, S.; Song, H.; Yang, G. C.; Zhang, L. J.; Ma, Y. M. *Phys. Rev. Lett.* **2016**, *116*, 057002.
(48) Wang, Y.; Lv, J.; Zhu, L.; Ma, Y. *Phys. Rev. B: Condens. Matter Mater. Phys.* **2010**, *82*, 094116.
(49) Wang, Y.; Lv, J.; Zhu, L.; Ma, Y. *Comput. Phys. Commun.* **2012**, *183*, 2063.
(50) Pickard, C. J.; Needs, R. J. *Phys. Rev. Lett.* **2006**, *97*, 045504.
(51) Oganov, A. R.; Glass, C. W. *J. Chem. Phys.* **2006**, *124*, 244704.
(52) Togo, A.; Oba, F.; Tanaka, I. *Phys. Rev. B: Condens. Matter Mater. Phys.* **2008**, *78*, 134106.
(53) Peng, F.; Miao, M.; Wang, H.; Li, Q.; Ma, Y. *J. Am. Chem. Soc.* **2012**, *134*, 18599.
(54) Lv, J.; Wang, Y.; Zhu, L.; Ma, Y. *Phys. Rev. Lett.* **2011**, *106*, 015503.
(55) Rousseau, B.; Xie, Y.; Ma, Y.; Bergara, A. *Eur. Phys. J. B* **2011**, *81*, 1.
(56) Atou, T.; Hasegawa, M.; Parker, L. J.; Badding, J. V. *J. Am. Chem. Soc.* **1996**, *118*, 12104.
(57) Takemura, K.; Fujihisa, H. *Phys. Rev. B: Condens. Matter Mater. Phys.* **2011**, *84*, 014117.
(58) Yang, G. C.; Wang, Y. C.; Ma, Y. M. *J. Phys. Chem. Lett.* **2014**, *5*, 2516.
(59) Zhu, L.; Wang, H.; Wang, Y.; Lv, J.; Ma, Y.; Cui, Q.; Ma, Y.; Zou, G. *Phys. Rev. Lett.* **2011**, *106*, 145501.
(60) Perdew, J. P.; Chevary, J. A.; Vosko, S. H.; Jackson, K. A.; Pederson, M. R.; Singh, D. J.; Fiolhais, C. *Phys. Rev. B: Condens. Matter Mater. Phys.* **1992**, *46*, 6671.
(61) Kresse, G.; Furthmuller, J. *Phys. Rev. B: Condens. Matter Mater. Phys.* **1996**, *54*, 11169.
(62) Courtney, I. A.; Tse, J. S.; Mao, O.; Hafner, J.; Dahn, J. R. *Phys. Rev. B: Condens. Matter Mater. Phys.* **1998**, *58*, 15583.
(63) Reuter, K.; Scheffler, M. *Phys. Rev. B: Condens. Matter Mater. Phys.* **2001**, *65*, 035406.
(64) Feng, J.; Hennig, R. G.; Ashcroft, N. W.; Hoffmann, R. *Nature* **2008**, *451*, 445.
(65) Togo, A.; Oba, F.; Tanaka, I. *Phys. Rev. B: Condens. Matter Mater. Phys.* **2008**, *78*, 134106.
(66) Blaha, P.; Schwarz, K.; Sorantin, P.; Trickey, S. B. *Comput. Phys. Commun.* **1990**, *59*, 399.

DOI: 10.1021/jacs.5b11768
J. Am. Chem. Soc. 2016, 138, 4046−4052

(67) Zhang, X.; Trimarchi, G.; Zunger, A. *Phys. Rev. B: Condens. Matter Mater. Phys.* **2009**, *79*, 092102.
(68) Pelton, A. D. *Bull. Alloy Phase Diagrams* **1986**, *7*, 228.
(69) Degtyareva, V. F. *Solid State Sci.* **2014**, *36*, 62.
(70) Ahuja, R.; Rekhi, S.; Johansson, B. *Phys. Rev. B: Condens. Matter Mater. Phys.* **2001**, *63*, 212101.
(71) Bishea, G.; Morse, M. *J. Chem. Phys.* **1991**, *95*, 5646.
(72) Schmidbaur, H. *Gold. Bull.* **2000**, *33*, 3.
(73) Dronskowski, R.; Blochl, P. E. *J. Phys. Chem.* **1993**, *97*, 8617.
(74) White, J. P.; Deng, H.; Boyd, E. P.; Gallucci, J.; Shore, S. G. *Inorg. Chem.* **1994**, *33*, 1685.
(75) Luo, X. L.; Baudry, D.; Boydell, P.; Charpin, P.; Nierlich, M.; Ephritikhine, M.; Crabtree, R. H. *Inorg. Chem.* **1990**, *29*, 1511.
(76) Simon, A. *Coord. Chem. Rev.* **1997**, *163*, 253.
(77) Hooper, J.; Zurek, E. *ChemPlusChem* **2012**, *77*, 969.
(78) Botana, J.; Miao, M. S. *Nat. Commun.* **2014**, *5*, 4861.
(79) Hernandez-Trujillo, J.; Bader, R. F. W. *J. Phys. Chem. A* **2000**, *104*, 1779.
(80) Becke, A. D.; Edgecombe, K. E. *J. Chem. Phys.* **1990**, *92*, 5397.
(81) Savin, A.; Jepsen, O.; Flad, J.; Andersen, O.; Preuss, H.; von Schnering, H. *Angew. Chem., Int. Ed. Engl.* **1992**, *31*, 187.
(82) Häussermann, U.; Wengert, S.; Hofmann, P.; Savin, A.; Jepsen, O.; Nesper, R. *Angew. Chem., Int. Ed. Engl.* **1994**, *33*, 2069.
(83) Pyykko, P. *J. Organomet. Chem.* **2006**, *691*, 4336.
(84) Kuznetsov, A. E.; Corbett, J. D.; Wang, L. S.; Boldyrev, A. I. *Angew. Chem., Int. Ed.* **2001**, *40*, 3369.
(85) Yong, L.; Chi, X. X. *J. Mol. Struct.: THEOCHEM* **2007**, *818*, 93.

DOI: 10.1021/jacs.5b11768
J. Am. Chem. Soc. 2016, 138, 4046−4052